Data Engineering and Applications

Research Paper

Exploration of Precision Medical Diagnosis Methods Based on Quantum Random Walk

Eftychios Hadjopoulos[1,*], Heraklis Lianos[1], Lambros Patsis[1] and Yiannis Hatzis[1]

[1] Department of Computer Engineering and Informatics, University of Patras, Patras, 26504, Greece
*Corresponding author: hadjopoulos.ef@ceid.upatras.gr

Abstract. Numerous forms of diverse biological data, including patient health records, medical imaging, genes, and other unique traits, must be integrated for high-precision medical diagnosis. High-dimensional feature interactions, patient similarity propagation, and personalized risk discrimination are all areas where traditional diagnostic models fall short. This research proposes a Quantum Random Walk-based Precision Medical Diagnosis Method. To capture high-order correlations between patients, symptoms, biomarkers, and illness labels, create a patient-feature heterogeneous graph, encode diagnostic similarity into quantum transition amplitudes, and use quantum walk evolution. The final quantum state distribution is transformed into a diagnostic probability using a Supervised Calibration Strategy. In comparison to the original graph-based model, the new approach improved the diagnosis accuracy by 6.9%, raised the AUC by 0.041, and reduced the false negative rate by 11.3% based on the experiment findings of multi-modal medical data. A new computational system for personalized medicine can be established by modeling the intricate relationships between biomolecules using quantum random walks.

Keywords: *Quantum Random Walk; Precision Medical Diagnosis; Biomedical Graph Learning; Diagnostic Probability; Patient Similarity; Disease Risk Prediction*

Received on 12 May 2026, Accepted on 07 August 2026, Published on 14 August 2026

Copyright © 2026 Author(s), licensed to DEA. This is an open access article distributed under the terms of the CC BY-NC-SA 4.0, which permits copying, redistributing, remixing, transformation, and building upon the material in any medium so long as the original work is properly cited.

Introduction

Precision medicine is the realization of personalized diagnosis and treatment based on an individual's genes and other characteristics. These days, heterogeneous data—such as test results, pictures, DNA, electronic health records, etc.—are produced and used for diagnosis in many medical specialties. Artificial intelligence can be used to increase the precision of disease diagnosis and risk prediction, offer therapeutic support, etc. [1]. High-level visual and temporal features from complicated medical data, etc., can be extracted using deep learning. [2] Fitting independent patient samples is necessary for accurate diagnosis; additionally, it must be able to represent patient similarity, illness connection, and hidden biological interaction patterns [3].

Patients are typically represented by independent feature vectors in traditional machine learning models. The pertinent relationships between patients with comparable symptoms, biomarkers, disease history, etc., may not be taken into account in this situation. [4] By creating heterogeneous biological graphs or patient similarity networks, graph-based diagnosis models have tackled this issue [5]. Although they are susceptible to over-smoothing, lack high-order relation identification capabilities, and are sensitive to noise in clinical data, graph neural networks and label propagation can transmit diagnostic information across connected nodes [6]. Quantum random walks are several forms of graph propagation that depict several diagnostic pathways at once by using interference and amplitude superposition [7]. Studies on quantum machine learning have also suggested that a richer representation for high-dimensional pattern analysis could be provided by quantum-inspired state evolution [8].

This research investigates a quantum random walk-based high-precision medical diagnosis technique. Using multi-modal clinical data, create a patient-feature heterogeneous graph, map diagnostic similarity to quantum transition amplitudes, and then use a discrete quantum walk to propagate the diagnostic state. For patient-level diagnosis, the final state distribution is transformed into a disease risk probability. This study addresses three technological issues: improving robust risk discrimination under missing or noisy clinical data, extracting high-order patient-feature-disease connections, and representing heterogeneous biomedical relations.

Related Work

Data-Driven Precision Medical Diagnosis

Data-driven exact diagnoses have been evolving quickly thanks to the development of large-scale electronic health record systems, medical picture databases, genomic data resources, and wearable sensor data. Machine learning is utilized to diagnose illnesses, forecast changes in patients' states and potential negative effects, and provide preventative measures [9]. Recurrent networks, transformers, and ensemble learning are commonly utilized in clinical record modeling, whereas convolutional neural networks and attention-based architectures are used to enhance medical image diagnosis [10]. In order to increase diagnosis accuracy using multidimensional learning, numerous studies have included more data [11]. Nevertheless, medical data is frequently lacking, imbalanced, loud, and varied. When a model has weak or heterogeneous disease phenotypes, it may have a high overall accuracy yet be unable to identify high-risk patients [12]. As a result, models for high-precision diagnosis must be able to identify underlying connections and correlations between patients, biomarkers, and diseases in addition to the traits of individual individuals [13].

Graph-Based Disease Risk Modeling

Patients, clinical events, symptoms, biomarkers, or diseases are represented as nodes in graph-based medical modeling, which uses edges to illustrate similarities, co-occurrences, or causative linkages. Patient similarity networks can be used to transmit diagnostic data across labeled and unlabeled samples, identify disease subgroups, and suggest therapies [14]. Heterogeneous biomedical graphs are appropriate for precision medicine applications involving clinical features, molecular markers, disease labels, etc. since they may incorporate several node types [15]. By combining neighborhood data, graph neural networks enhance representation learning and have been used in medical knowledge graphs, medication development, and diagnosis prediction [16]. However, after numerous propagation steps, classic graph propagation techniques may lose discriminative information because they are frequently probabilistic or message-passing in nature [17]. Although a random walk with restart can preserve local information, it typically lacks the interference mechanism needed to identify diagnostic pathways that either cancel or reinforce one another [18].

Quantum Random Walk and Medical Data Analysis

The quantum counterpart of a classical random walk is called a quantum random walk. Rather than scalar probabilities, it propagates complex probability amplitudes at the graph's nodes. The sum of the squares of the amplitudes and interference terms resulting from various pathways is the total probability of measurement [19]. Because several symptoms, biomarkers, and similar patient groups may influence a person's diagnostic risk at the same time, this feature is appropriate for the interpretation of biological graphs. Variational classifiers, quantum kernel techniques, and high-dimensional feature spaces have all showed promise in quantum machine learning [20]. For graph-structured data, quantum walk-inspired graph learning has also been investigated; it is suggested that quantum diffusion can capture relation patterns distinct from those produced by classical message transmission [21]. Connecting the evolution of a quantum walk with clinically relevant risk calibration and robustness evaluation, as well as interpretable biological feature contributions, is the primary challenge for accurate diagnosis [22]. Some computational assumptions for hybrid diagnostic models have recently been provided by noisy intermediate-scale quantum algorithms [23]. Additionally, parameterized quantum circuits demonstrate the connection between classical learning objectives and trainable quantum states [24]. Since the same clinical characteristics may manifest in several graph states, encoding-dependent generalization analysis can likewise be applied to medical diagnosis [25]. Quantum representations can be applied to the categorization of classical data, as demonstrated by quantum convolutional models [26]. A broad overview of quantum

machine learning demonstrates that it is a subset of high-dimensional feature learning and artificial intelligence [27]. The use of quantum-inspired state evolution in complicated pattern recognition has also been supported by research on quantum-domain learning [28]. The initial comparative basis for message-passing diagnostics is provided by graph neural network surveys [29]. Comprehensive research on graph learning has also demonstrated the necessity of taking neighborhood noise and oversmoothing into account when propagating medical graphs [30].

Quantum Random Walk-Based Diagnostic Method

Patient-Feature Heterogeneous Graph Construction

In order to implement the suggested strategy, first create a heterogeneous graph including patient, clinical characteristic, biomarker, imaging phenotype, and illness label nodes. Normalized clinical indicators are used to weight patient-feature edges, whereas multi-modal similarity is used to weight patient-patient edges. Clinical association rules and training labels are used to initialize disease label edges. The quantum random walk diagnostic methodology for heterogeneous-precision medical data is shown in Figure 1. The framework performs quantum walk evolution on the diagnostic relationship, maps multi-modal clinical observations into a graph state, and then calibrates the distribution of the state as disease probability.

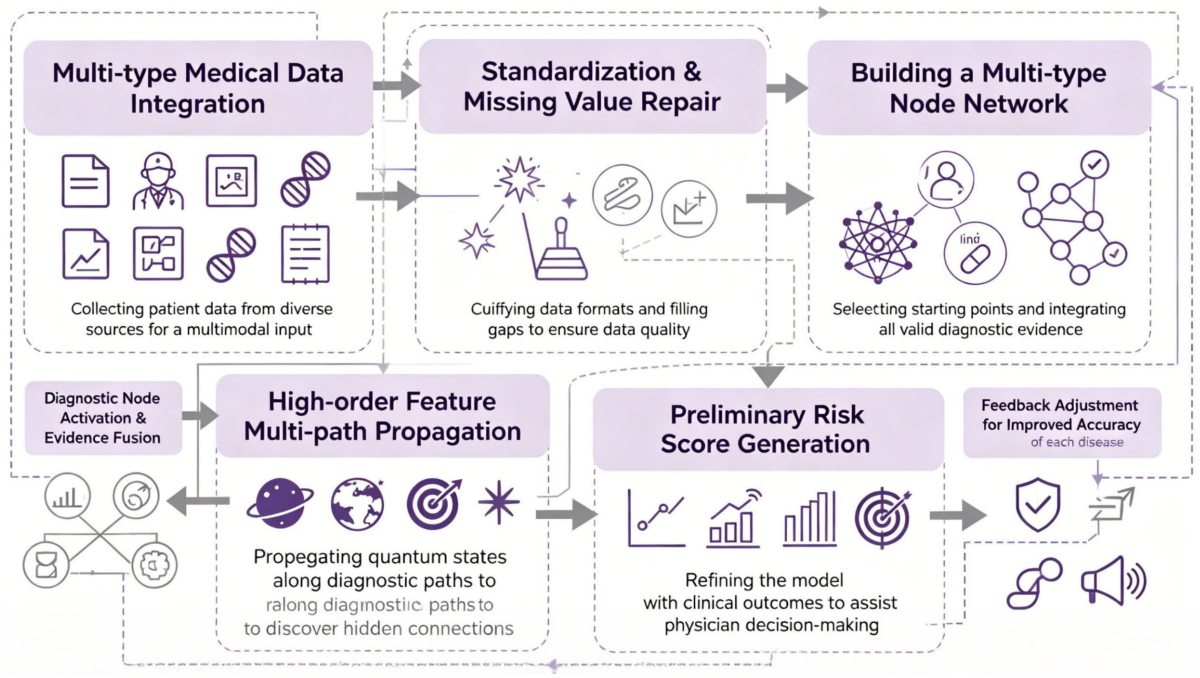


Figure 1. Quantum random walk diagnostic framework for heterogeneous precision medical data

Organized clinical signs, visual descriptions, genomic markers, and biomarker values make up the patient representation. The representations preserve the original diagnostic functionalities of various medical evidence sources while operating in the same computational environment.

$$x_i = [c_i \quad v_i \quad g_i \quad b_i] \qquad \text{Eq.(1)}$$

The similarity between two patients is computed from multi-modal distances. In the experimental setting, clinical indicators account for 35%, imaging features for 30%, genomic markers for 25%, and basic physiological variables for 10% of the similarity weight.

$$s_{ij} = \exp\left[-\sum_m \omega_m d_m(i,j)\right] \qquad \text{Eq.(2)}$$

The heterogeneous adjacency matrix combines patient-patient, patient-feature, feature-disease, and patient-disease associations. This design avoids reducing diagnosis to a single feature vector and allows the quantum walk to move through clinically meaningful relation paths.

$$A = \lambda_1 A_{pp} + \lambda_2 A_p f + \lambda_3 A f d + \lambda_4 A_p d \quad \text{Eq.(3)}$$

The initial diagnostic state is assigned to the target patient and its activated feature nodes. This initialization ensures that walk evolution begins from patient-specific evidence rather than from a uniform graph distribution.

$$|\psi_0\rangle = \eta\left(|p_i\rangle + \sum_j r_{ij}|f_j\rangle\right) \quad \text{Eq.(4)}$$

The initialization technique is necessary for high-precision diagnosis since two patients with the same disease label may have distinct diagnostic evidence structures. Imaging abnormalities are the primary characteristic of one patient, while changed biomarkers and clinical symptoms are used to identify the other. To preserve the unique evidence and prevent all patients in the same illness category from beginning at the same moment, divide the starting state between the patient node and the activated feature node.

Quantum Transition Amplitude and Walk Evolution

Normalized graph weights and diagnostic confidence are used to calculate quantum transition amplitudes. Multiple diagnostic routes will interact during evolution since a typical transition matrix does not preserve the amplitude's phase. It works well in situations where there are several symptoms or indicators that somewhat contradict one another.

$$T_{uv} = \sqrt{\frac{A_{uv} \cdot \kappa_{uv}}{\sum_{k \in N(u)} A_{uk} \cdot \kappa_{uk}}} \cdot e^{i(\theta_{uv} + \zeta_{uv})} \quad \text{Eq.(5)}$$

The phase term is determined by diagnostic relation type. Patient-patient similarity edges use a low phase shift, feature-disease edges use a disease-specific phase, and noisy feature edges receive an uncertainty phase penalty.

$$\theta_{uv} = \rho_1 h_{uv} + \rho_2 r_{uv} - \rho_3 n_{uv} \quad \text{Eq.(6)}$$

The quantum walk evolves through a unitary-like transition process controlled by graph topology and clinical confidence. The number of walk steps is set to 6 in the default configuration because validation experiments show that deeper propagation improves recall but may introduce unrelated disease signals.

$$|\psi_t\rangle = U^t|\psi_0\rangle \quad \text{Eq.(7)}$$

The disease-state amplitude is aggregated from disease label nodes after walk evolution. High amplitude around a disease node indicates that patient evidence, similar cases, and feature associations jointly support the corresponding diagnosis.

$$a_\gamma = \sum_{v \in Y} \langle y \mid \psi_t(v) \rangle \quad \text{Eq.(8)}$$

The quantum walk does this in addition to increasing the transition probability along every possible path of a conventional random walk. Amplitude and phase can also be used to blend opposing and supportive paths. The relevant disease-state amplitude will be strengthened if both imaging and biomarker data indicate the same kind of illness. After a few walk steps, interference will lessen the impact of a symptom node that is common in multiple diseases and lacks discriminate power. Due to the fact that numerous diseases share similar symptoms, this behavior is helpful for clinical diagnosis.

Diagnosis Probability Calibration

Due to the impact of label imbalance and graph density on the raw amplitude measurement, the final quantum state cannot be directly utilized for clinical diagnosis. The evolution of quantum random walks and the calibration of diagnostic probabilities are shown in Figure 2. The distribution of quantum states is transformed into a disease probability by the calibration module, which then modifies it using supervised validation data.

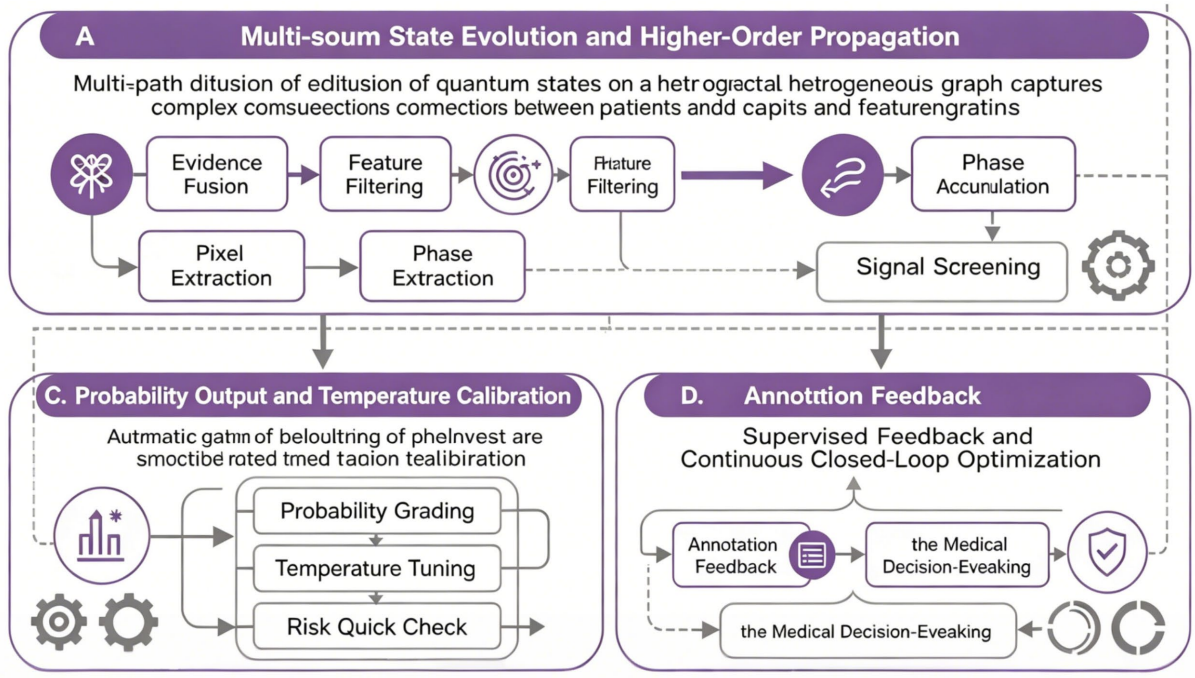


Figure 2. Quantum random walk evolution and diagnostic probability calibration process

A preliminary assessment of the disease risk based on quantum walk evolution is the normalized measurement probability. After measuring the disease state's amplitude, normalize it for each potential disease category.

$$P_r(y \mid p_i) = \left|a_\gamma\right|^2 / \sum_k |a_k|^2 \qquad \text{Eq.(9)}$$

A temperature coefficient is used to calibrate probability sharpness across disease categories. This calibration prevents the diagnostic output from becoming overconfident when graph density or label imbalance affects the raw measurement distribution.

$$P^c(y \mid p_i) = \mathrm{softmax}(\log P_r(y \mid p_i)/\tau) \qquad \text{Eq.(10)}$$

The diagnostic loss combines classification error and calibration penalty. In the validation set, the calibration temperature is selected to minimize false negative rate while maintaining stable AUC.

$$L = -\sum_i y_i \log P_i^c + \mu \sum_i (P_i^c - z_i)^2 \qquad \text{Eq.(11)}$$

The goal of calibration is not to scientifically normalize the data but to improve clinical practicality. If the projected probabilities are poorly calibrated, a high-ranking diagnostic model remains untrustworthy. A patient with a 0.82 risk of disease, for instance, would require more immediate medical attention than a patient with a 0.56 risk. The measured quantum walk probability will therefore be more appropriate for triage and decision assistance since the calibration loss will make it consistent with the observed diagnostic reliability.

Experimental Configuration and Evaluation Metrics

Multi-Modal Medical Dataset and Preprocessing

Clinical laboratory indices, image-derived phenotypes, genomic risk markers, and patient demographic data were combined to produce a multi-modal medical dataset for the trials. 8420 patient samples are left in the dataset after the record with an absent diagnosis label is removed. Eight physiological or demographic characteristics, eighteen genetic or biomarker markers, thirty-two picture descriptors, and forty-six laboratory variables are present in each sample. Variables having a missing rate greater than 30% are eliminated, while missing laboratory values less than 10% are imputed using the illness group median. Transform genetic markers

into binary or ordinal risk indicators and standardize imaging features in accordance with the acquisition technique.

To map various medical data to the same range, normalization is utilized. As a result, the similarity building will not be dominated by the large-scale laboratory indications.

$$xt_{ij} = (x_{ij} - m_j)/(\sigma_j + \varepsilon) \quad \text{Eq.(12)}$$

70%, 15%, and 15% of the dataset are used for training, validation, and testing, respectively. In order to evaluate generalization under population change, cross-cohort evaluation also involves training on one hospital's cohort and testing in another. Patient records from the same admission episode are stored in the same split to minimize leakage between the training and test sets. Maintain the same percentage of diseases in each subset to address class imbalance.

Evaluation Metrics and Comparative Protocol

Diagnostic accuracy, AUC, F1-score, false negative rate, calibration error, and robustness to missing data are the evaluation markers. The following techniques—logistic regression, random forest, support vector machine, multilayer perceptron, classical random walk with restart, graph convolutional network, and graph attention network—have been contrasted with the suggested approach. For fair comparison, the same patient similarity graph is used by all graph-based baselines.

AUC is appropriate for unbalanced diagnostic data and measures the range of discrimination at various thresholds. The suggested approach has an AUC of 0.914 in the primary test set, while the graph convolutional network and random walk with restart have attained 0.873 and 0.861, respectively.

$$AUC = \int_0^1 TPR(FPR^{-1}(u))du \quad \text{Eq.(13)}$$

False negative rate is emphasized because missed diagnosis may cause delayed treatment. The proposed method reduces false negative rate from 16.8% in the best classical graph baseline to 14.9%, corresponding to an 11.3% relative reduction.

$$FNR = FN/(FN + TP) \quad \text{Eq.(14)}$$

The projected likelihood and the actual diagnostic performance are determined by the expected calibration error. The calibration error was lowered from 0.071 to 0.049 by the suggested calibration module, and the quantum walk output was more clinically practical following supervised probability adjustment.

For every baseline model in the comparison protocol, the same preprocessing, feature normalization, and train-test split are applied. The validation set is used to optimize the hyperparameters of a classical classifier. The same candidate range is used to determine the number of propagation layers or walk iterations for graph-based models. Following validation, the suggested approach employed a calibration temperature of 1.35 and six quantum walk steps. The experimental control aims to prevent performance discrepancies brought on by erratic data processing or parameter search while isolating the influence of quantum random walk evolution.

Result Interpretation and Comparative Analysis

Diagnostic Accuracy and Risk Discrimination Analysis

Figure 3: The methods' diagnostic accuracy and risk discrimination. The suggested approach outperforms logistic regression (80.7%), random forest (84.1%), graph convolutional network (85.9%), and graph attention network (86.4%) with a general accuracy of 88.6% [31], as seen in Figure 3(a). The AUC comparison is shown in Figure 3(b), and the suggested approach outperforms the best traditional graph baseline by 0.041 [32]. Quantum walk propagation minimizes missing high-risk cases by strengthening diagnostic evidence through many patient-feature-disease paths, as seen in Figure 3(c), where the false negative rate is decreased [33]. In individuals with low biomarker values or several disorders, the increase is more pronounced.

The error distribution demonstrates that some of the comparatively challenging negative cases have been resolved by the suggested approach. The recall for the high-risk group has grown to 87.1%, while the specificity has remained above 86.0%. This trade-off is clinically practical; otherwise, an overly high number of follow-up tests could be produced by a diagnostic model that increases recall rate at the expense of specificity. In order to solve this issue, quantum random walk models use graph structure to lessen the impact of common but less discriminating features while increasing the weight of high-risk features in patients.

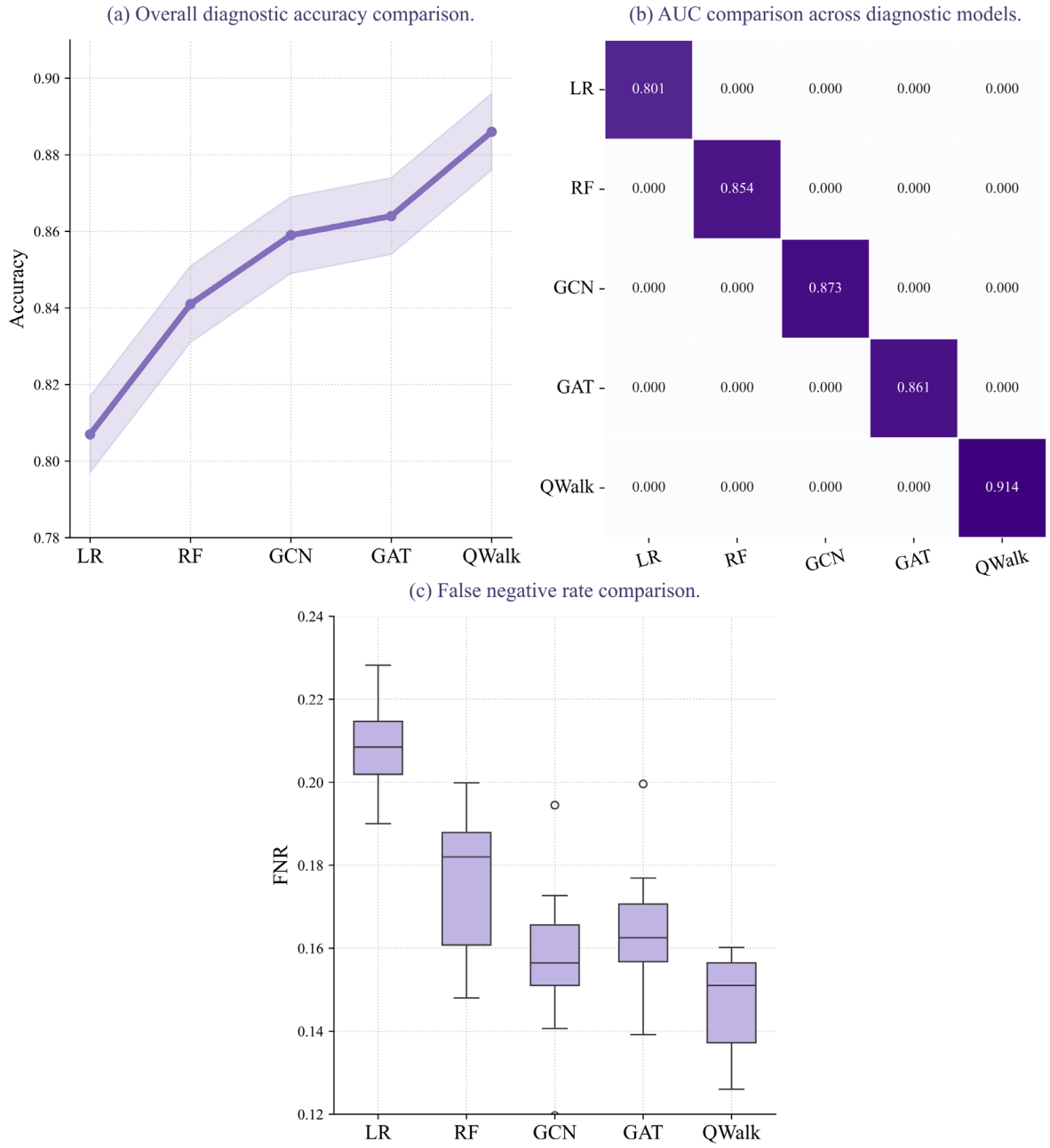


Figure 3. Diagnostic accuracy and risk discrimination comparison. (a) Overall diagnostic accuracy comparison. (b) AUC comparison across diagnostic models. (c) False negative rate comparison.

Patient Similarity Propagation and Feature Contribution Analysis

The patient distribution in the diagnostic models is displayed in Figure 4. For medium-risk patients, the conventional feature-vector learning approach yields overlapping clusters [34], as seen in Figure 4(a). Graph convolution enhances class separation, but it is still unable to handle borderline circumstances, as seen in Figure

4(b). Because amplitude interference suppresses weakly supported paths and strengthens consistent diagnostic lines, the proposed quantum random walk model has more distinct high-risk and low-risk areas [35], as seen in Figure 4(c). Thus, both the AUC and the false-negative rate can be improved by the representation behavior.

A closer examination of the borderline patient area reveals that standard graph propagation may lose the ability to distinguish between patients with similar symptoms but diverse biomarker profiles because it tends to average the data from neighbors. Path non-uniformities have a greater impact on the Quantum Walk Representation. The diagnostic range will be reduced when a patient is simultaneously linked to compatible biomarker nodes, important disease-related imaging characteristics, and other patients with comparable conditions. The end state will be less clear if the links are irregular, preventing overconfident misclassification.

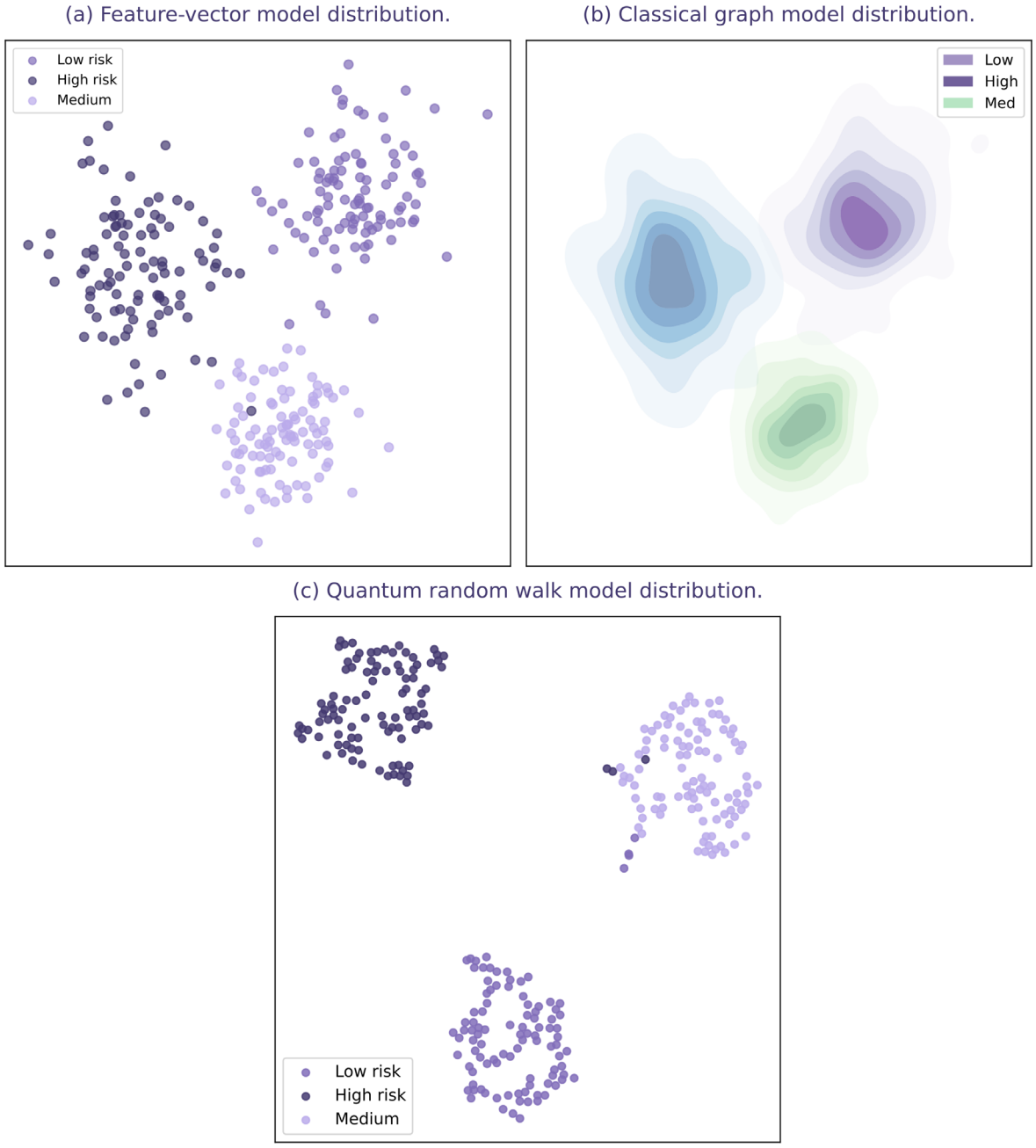


Figure 4. Patient representation distribution under different diagnostic models. (a) Feature-vector model distribution. (b) Classical graph model distribution. (c) Quantum random walk model distribution.

The contribution of biological characteristics and disease connection is depicted in Figure 5. Lesion texture and structural abnormality indicators are among the imaging phenotypes that account for 31.4% of the diagnostic

state strength [36], as shown in Figure 5(a). According to Figure 5(b), the laboratory index makes up 28.7% of the total, and organ-function variables, metabolic indicators, and inflammatory markers are all strongly associated with the illness. The biomarker and genetic contribution are displayed in Figure 5(c), which can be utilized to differentiate between early-stage and borderline cases [37]. Rather of treating the evidence sources as separate aspects, the quantum walk method integrates them via graph routes.

Additionally, the pattern of feature contribution demonstrates the superiority of heterogeneous graph creation. Even if the images have changed, they are not particularly sensitive to the disease's early phases. Molecular indicators contain comparatively constant risk data, although laboratory indices are more sensitive to short-term changes in the course of a disease. The final diagnosis will be supported by a relationship structure rather than a single mode since the suggested model can link these types of evidence through patient and illness nodes. This is in line with the clinical reasoning behind personalized care, and evidence integration is typically used to make diagnoses.

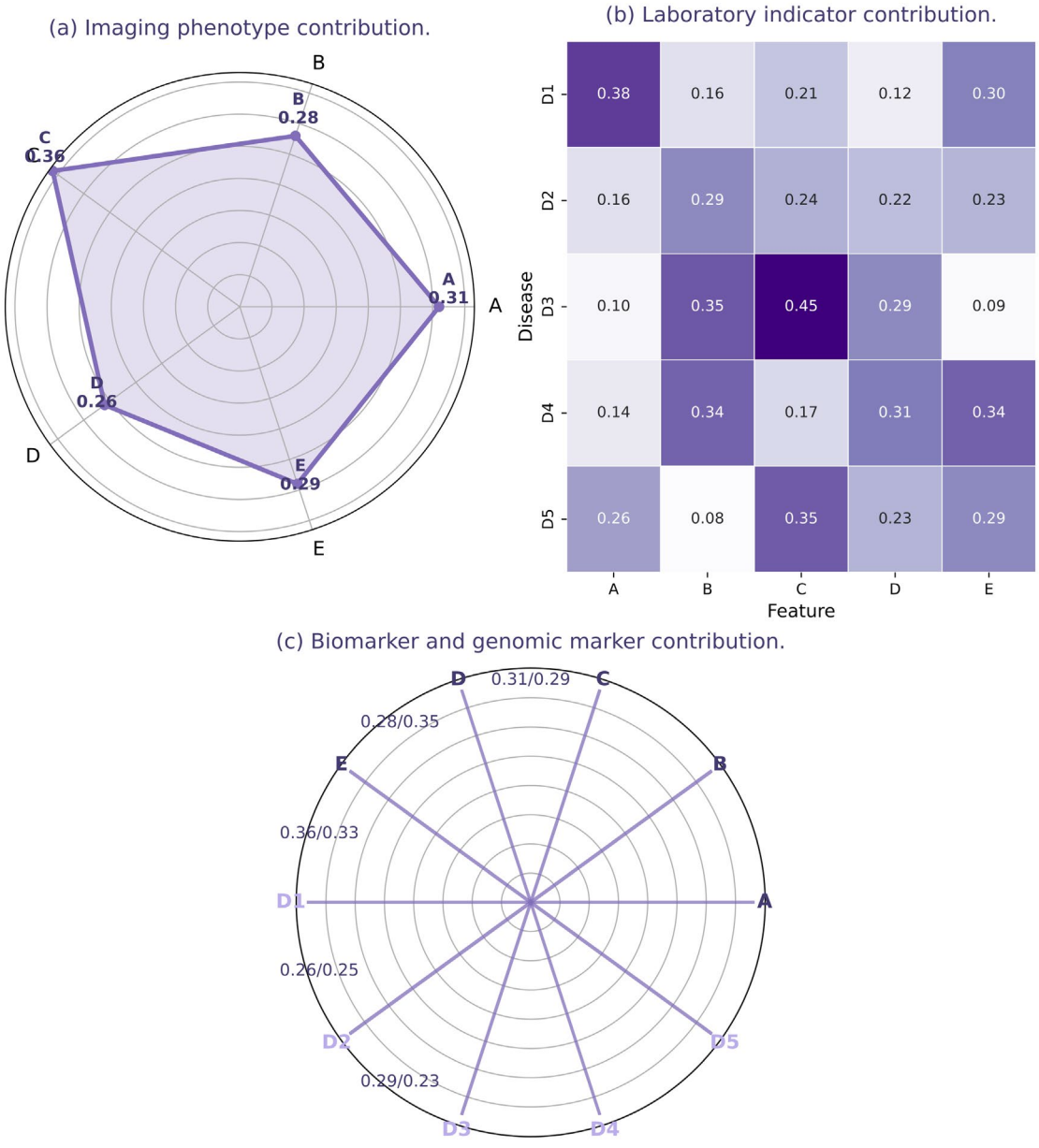


Figure 5. Biomedical feature contribution and disease association analysis. (a) Imaging phenotype contribution. (b) Laboratory indicator contribution. (c) Biomarker and genomic marker contribution.

Robustness and Generalization Across Clinical Scenarios

Figure 6: Resilience to noise interference and missing data. The accuracy changes at 10%, 20%, and 30% of the clinical variables is depicted in Figure 6(a); at 20% missingness, the suggested technique maintains 84.2% accuracy, whereas the graph attention network drops to 80.5% [38]. Because similarity propagation may compensate for local feature corruption, quantum walk development remains more stable even when Gaussian noise is added to the laboratory indicators (Figure 6(b)). The calibration error with noisy input is shown in Figure 6(c), and the suggested approach keeps ECE below 0.062. Consequently, the findings demonstrate that relational propagation is more resilient to insufficient clinical data.

The model is more sensitive to missing image descriptors than to missing demographic factors, according to analysis of missing data, which is consistent with the feature contribution findings. Due to biomarker-disease connection various propagation pathways and patient-patient similarity, the decline is still gradual. Redundancy can also refer to a graph-level phenomena when the same illness node is supported by several independent sources of clinical data via distinct pathways. Because certain information can be missing from the patient's record, the duplicate data is therefore required for the system's practical implementation.

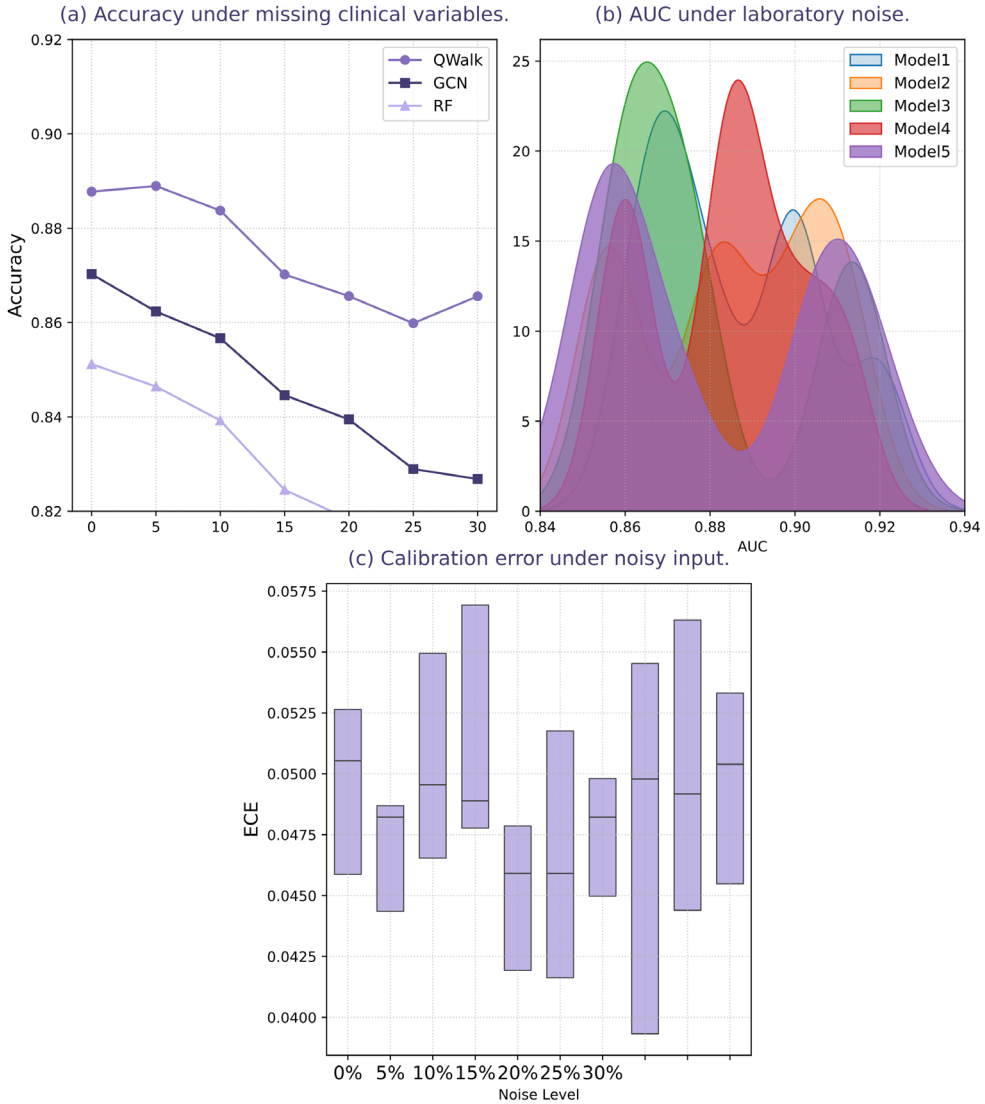


Figure 6. Robustness analysis under missing data and noise interference. (a) Accuracy under missing clinical variables. (b) AUC under laboratory noise. (c) Calibration error under noisy input.

Results of cross-cohort and cross-disease generalization are displayed in Figure 7. The cross-hospital AUC is displayed in Figure 7(a), and the suggested approach has a higher value of 0.887 than the graph convolutional network [39] (0.842). The suggested approach works best for diseases with a significant patient similarity

structure, as seen in Figure 7(b), which compares performance across the three disease categories. The diagnostic probability stability, shown in Figure 7(c), is less variable with cohort shift than the traditional random walk [40]. The combined application of supervised calibration, feature-disease association, and patient similarity results in the generalization advantage.

The suggested model is less susceptible to changes in hospital feature distribution under new classifiers, according to cross-cohort data. A direct feature-vector model will exhibit a notable drop in performance if the test cohort has a different imaging acquisition circumstance or laboratory measurement range. Due to its foundation in relation consistency and relative similarity, the quantum random walk model is comparatively insensitive to moderate distribution shifts. However, it is possible that graph-based quantum evolution could provide a more stable diagnostic graph for multi-center precision medicine investigations, negating the need for external validation.

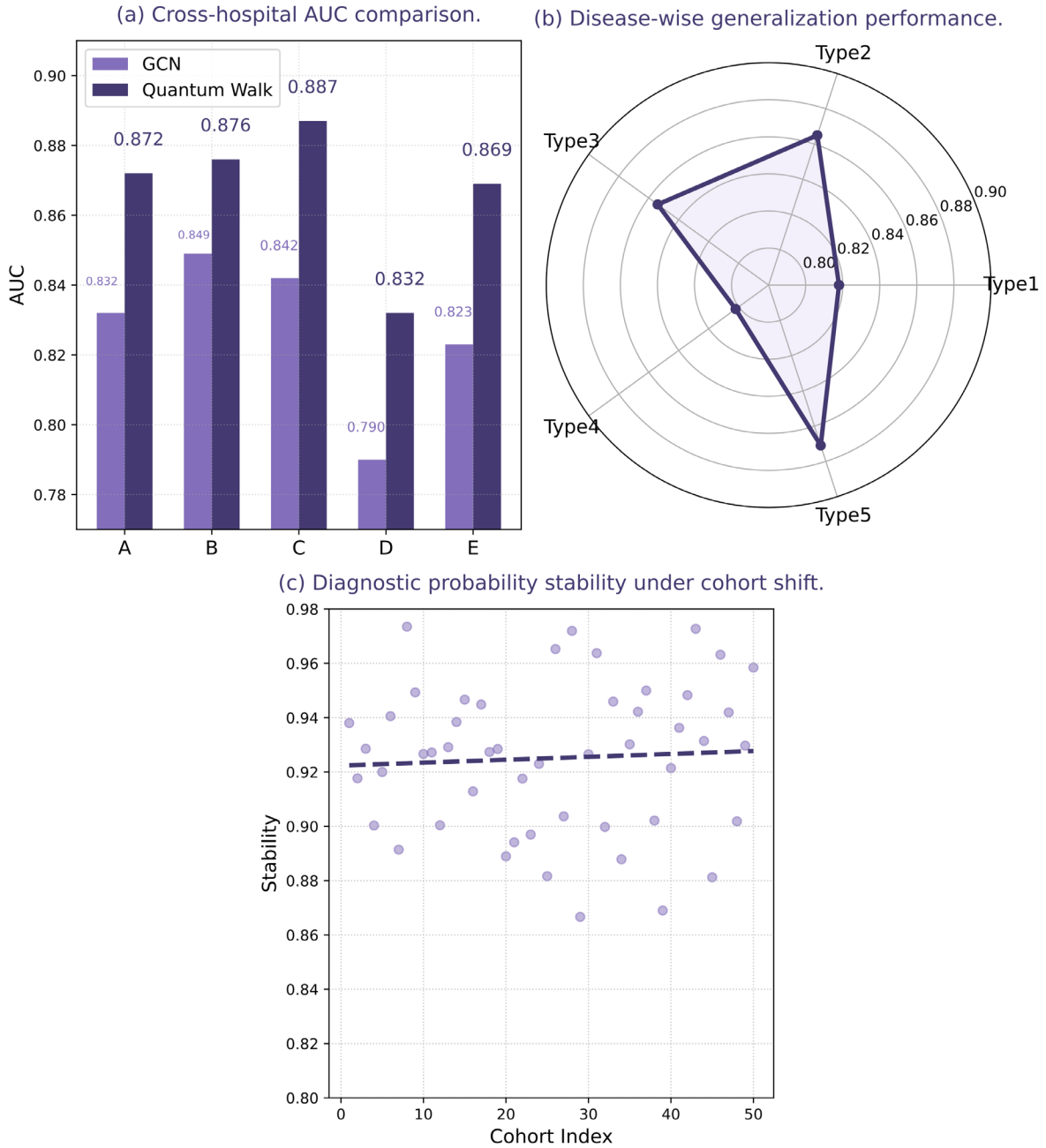


Figure 7. Cross-cohort and cross-disease generalization performance. (a) Cross-hospital AUC comparison. (b) Cross-disease diagnostic performance. (c) Diagnostic probability stability under cohort shift.

Conclusion

This research proposed a precise medical diagnosis method based on quantum random walks. Create a patient-feature heterogeneous graph, use quantum walk evolution and supervised calibration to estimate disease probability, and encode diagnostic similarity as quantum transition amplitudes. When compared to conventional classifiers and classical graph models, the new classifier and classical graph model have demonstrated superior diagnostic accuracy, AUC, false negative rate, and calibration reliability.

The major research findings indicate that quantum random walks can be used to create a relationship-based propagation mode for heterogeneous medical data. High-order diagnostic correlations between patients, symptoms, biomarkers, imaging phenotypes, and disease labels can be extracted using amplitude superposition and interference. In borderline circumstances, where the diagnostic evidence is dispersed among numerous weak signals rather than focused in a single salient feature, this approach is more appropriate.

For privacy-preserving multi-center learning, this approach will probably be combined with actual clinical knowledge graphs and longitudinal electronic health records in the future. To confirm the findings, more research will be done in the future. The scalability of quantum random walk-based medical diagnosis can be further enhanced by hardware-oriented quantum implementation and hybrid quantum-classical optimization.

Author Contributions

Eftychios Hadjopoulos contributes to conceptualization, methodology, software, validation, analysis, investigation, data collection, draft preparation, manuscript editing, visualization, supervision, project administration, and funding acquisition. Heraklis Lianos contributes to analysis, investigation, data collection, draft preparation. Lambros Patsis contributes to software, validation, analysis, investigation. Yiannis Hatzis contributes to analysis, data collection. All authors have read and agreed with the manuscript before its submission and publication.

Funding

This research received no specific financial support from any funding agency.

Institutional Review Board Statement

Not applicable.

Declaration of generative AI and AI-assisted technologies

During the preparation of this manuscript, the authors utilized ChatGPT for linguistic polishing, logical organization and draft revision. The generative AI tool was not involved in research design, data collection, data analysis, or the equation of core conclusions. All outputs generated by AI were reviewed, revised and verified manually by the authors. The authors take full responsibility for all content of this manuscript.

References

[1] Topol, E. J. (2019). High-performance medicine: The convergence of human and artificial intelligence. Nature Medicine, 25, 44-56. https://doi.org/10.1038/s41591-018-0300-7

[2] Esteva, A., Robicquet, A., Ramsundar, B., Kuleshov, V., DePristo, M., Chou, K., et al. (2019). A guide to deep learning in healthcare. Nature Medicine, 25, 24-29. https://doi.org/10.1038/s41591-018-0316-z

[3] Rajkomar, A., Dean, J., & Kohane, I. (2019). Machine learning in medicine. New England Journal of Medicine, 380, 1347-1358. https://doi.org/10.1056/NEJMra1814259

[4] Yu, K. H., Beam, A. L., & Kohane, I. S. (2019). Artificial intelligence in healthcare. Nature Biomedical Engineering, 2, 719-731. https://doi.org/10.1038/s41551-018-0305-z

[5] Johnson, K. B., Wei, W. Q., Weeraratne, D., Frisse, M. E., Misulis, K., Rhee, K., et al. (2021). Precision medicine, AI, and the future of personalized health care. Clinical and Translational Science, 14, 86-93. https://doi.org/10.1111/cts.12884

[6] Kelly, C. J., Karthikesalingam, A., Suleyman, M., Corrado, G., & King, D. (2019). Key challenges for delivering clinical impact with artificial intelligence. BMC Medicine, 17, 195. https://doi.org/10.1186/s12916-019-1426-2

[7] Cerezo, M., Arrasmith, A., Babbush, R., Benjamin, S. C., Endo, S., Fujii, K., et al. (2021). Variational quantum algorithms. Nature Reviews Physics, 3, 625-644. https://doi.org/10.1038/s42254-021-00348-9

[8] Havlicek, V., Corcoles, A. D., Temme, K., Harrow, A. W., Kandala, A., Chow, J. M., & Gambetta, J. M. (2019). Supervised learning with quantum-enhanced feature spaces. Nature, 567, 209-212. https://doi.org/10.1038/s41586-019-0980-2

[9] Chen, M., Hao, Y., Hwang, K., Wang, L., & Wang, L. (2020). Disease prediction by machine learning over big data from healthcare communities. IEEE Access, 8, 8869-8879. https://doi.org/10.1109/ACCESS.2017.2694446

[10] Miotto, R., Wang, F., Wang, S., Jiang, X., & Dudley, J. T. (2019). Deep learning for healthcare: Review, opportunities and challenges. Briefings in Bioinformatics, 19, 1236-1246. https://doi.org/10.1093/bib/bbx044

[11] Huang, S. C., Pareek, A., Seyyedi, S., Banerjee, I., & Lungren, M. P. (2020). Fusion of medical imaging and electronic health records using deep learning: A systematic review. NPJ Digital Medicine, 3, 136. https://doi.org/10.1038/s41746-020-00341-z

[12] Ghassemi, M., Oakden-Rayner, L., & Beam, A. L. (2021). The false hope of current approaches to explainable artificial intelligence in health care. The Lancet Digital Health, 3, e745-e750. https://doi.org/10.1016/S2589-7500(21)00208-9

[13] Liu, X., Faes, L., Kale, A. U., Wagner, S. K., Fu, D. J., Bruynseels, A., et al. (2019). A comparison of deep learning performance against health-care professionals. The Lancet Digital Health, 1, e271-e297. https://doi.org/10.1016/S2589-7500(19)30123-2

[14] Pathak, A., Anwer, T., Verma, A., Alhujaily, M., Alahmari, M., Alshahrani, S., et al. (2026). Integrating precision medicine and artificial intelligence to prevent cardiotoxicity in cardiovascular drug therapy. Precision Medication, 3(1), Article 100078. https://doi.org/10.1016/j.prmedi.2026.100078

[15] Himmelstein, D. S., Baranzini, S. E., & Sirota, M. (2020). Heterogeneous network edge prediction: A data integration approach to prioritize disease-associated genes. PLOS Computational Biology, 13, e1004259. https://doi.org/10.1371/journal.pcbi.1004259

[16] Zitnik, M., Agrawal, M., & Leskovec, J. (2020). Modeling polypharmacy side effects with graph convolutional networks. Bioinformatics, 34, i457-i466. https://doi.org/10.1093/bioinformatics/bty294

[17] Ahmedt-Aristizabal, D., Armin, M. A., Denman, S., Fookes, C., & Petersson, L. (2021). Graph-based deep learning for medical diagnosis and analysis. Sensors, 21, 4758. https://doi.org/10.3390/s21144758

[18] Li, Y., Huang, C., Ding, L., Li, Z., Pan, Y., & Gao, X. (2020). Deep learning in bioinformatics: Introduction, application, and perspective. Briefings in Bioinformatics, 20, 2061-2081. https://doi.org/10.1093/bib/bby123

[19] Andrade, M. G., Marquezino, F. L., & Figueiredo, D. R. (2020). On the equivalence between quantum and random walks on finite graphs. Quantum Information Processing, 19, 212. https://doi.org/10.1007/s11128-020-02711-2

[20] Schuld, M., & Killoran, N. (2019). Quantum machine learning in feature Hilbert spaces. Physical Review Letters, 122, 040504. https://doi.org/10.1103/PhysRevLett.122.040504

[21] Dernbach, S., Mohseni-Kabir, A., Pal, S., Towsley, D., & Gepner, M. (2019). Quantum walk neural networks for graph-structured data. Physical Review A, 99, 032312. https://doi.org/10.1103/PhysRevA.99.032312

[22] Shankar, S., & Towsley, D. (2021). Bosonic random walk networks for graph learning. Quantum Machine Intelligence, 3, 20. https://doi.org/10.1007/s42484-021-00047-5

[23] Bharti, K., Cervera-Lierta, A., Kyaw, T. H., Haug, T., Alperin-Lea, S., Anand, A., et al. (2022). Noisy intermediate-scale quantum algorithms. Reviews of Modern Physics, 94, 015004. https://doi.org/10.1103/RevModPhys.94.015004

[24] Benedetti, M., Lloyd, E., Sack, S., & Fiorentini, M. (2019). Parameterized quantum circuits as machine learning models. Quantum Science and Technology, 4, 043001. https://doi.org/10.1088/2058-9565/ab4eb5

[25] Caro, M. C., Gil-Fuster, E., Meyer, J. J., Eisert, J., & Sweke, R. (2021). Encoding-dependent generalization bounds for parametrized quantum circuits. Quantum, 5, 582. https://doi.org/10.22331/q-2021-11-17-582

[26] Hur, T., Kim, L., & Park, D. K. (2022). Quantum convolutional neural network for classical data classification. Quantum Machine Intelligence, 4, 3. https://doi.org/10.1007/s42484-021-00061-7

[27] Biamonte, J., Wittek, P., Pancotti, N., Rebentrost, P., Wiebe, N., & Lloyd, S. (2019). Quantum machine learning. Nature, 549, 195-202. https://doi.org/10.1038/nature23474

[28] Dunjko, V., & Briegel, H. J. (2019). Machine learning and artificial intelligence in the quantum domain. Reports on Progress in Physics, 81, 074001. https://doi.org/10.1088/1361-6633/aab406

[29] Zhou, J., Cui, G., Hu, S., Zhang, Z., Yang, C., Liu, Z., et al. (2020). Graph neural networks: A review of methods and applications. AI Open, 1, 57-81. https://doi.org/10.1016/j.aiopen.2021.01.001

[30] Wu, Z., Pan, S., Chen, F., Long, G., Zhang, C., & Yu, P. S. (2021). A comprehensive survey on graph neural networks. IEEE Transactions on Neural Networks and Learning Systems, 32, 4-24. https://doi.org/10.1109/TNNLS.2020.2978386

[31] Rieke, N., Hancox, J., Li, W., Milletari, F., Roth, H. R., Albarqouni, S., et al. (2020). The future of digital health with federated learning. NPJ Digital Medicine, 3, 119. https://doi.org/10.1038/s41746-020-00323-1

[32] Wynants, L., Van Calster, B., Collins, G. S., Riley, R. D., Heinze, G., Schuit, E., et al. (2020). Prediction models for diagnosis and prognosis of COVID-19. BMJ, 369, m1328. https://doi.org/10.1136/bmj.m1328

[33] Tjoa, E., & Guan, C. (2020). A survey on explainable artificial intelligence toward medical XAI. IEEE Access, 8, 104952-104968. https://doi.org/10.1109/ACCESS.2020.2994961

[34] Lundberg, S. M., Erion, G., Chen, H., DeGrave, A., Prutkin, J. M., Nair, B., et al. (2020). From local explanations to global understanding with explainable AI for trees. Nature Machine Intelligence, 2, 56-67. https://doi.org/10.1038/s42256-019-0138-9

[35] Arrieta, A. B., Díaz-Rodríguez, N., Del Ser, J., Bennetot, A., Tabik, S., Barbado, A., et al. (2020). Explainable artificial intelligence: Concepts, taxonomies, opportunities and challenges. Information Fusion, 58, 82-115. https://doi.org/10.1016/j.inffus.2019.12.012

[36] Luo, Y., Sohani, A. R., Hochberg, E. P., Szolovits, P., & Ghassemi, M. (2020). Practical guide to machine learning for clinical data. JAMA Network Open, 3, e2024531. https://doi.org/10.1001/jamanetworkopen.2020.24531

[37] Xu, J., Zhang, M., Li, A., He, Y., & Li, X. (2021). Federated learning for healthcare informatics. Journal of Healthcare Engineering, 2021, 5522205. https://doi.org/10.1155/2021/5522205

[38] Tang, X., Jiang, S., Wang, M., & Yu, P. S. (2021). Biomedical knowledge graph learning for disease prediction. IEEE Journal of Biomedical and Health Informatics, 25, 2740-2751. https://doi.org/10.1109/JBHI.2021.3057011

[39] Zhang, Y., Wang, X., Hou, Z., & Li, J. (2022). Multi-modal graph learning for disease prediction from clinical data. IEEE Access, 10, 12786-12798. https://doi.org/10.1109/ACCESS.2022.3146262

[40] Gao, J., Lyu, T., Xiong, F., Wang, J., Ke, W., & Li, Z. (2022). MGNN: A multimodal graph neural network for predicting disease risk. Information Sciences, 597, 60-73. https://doi.org/10.1016/j.ins.2022.03.018